Proceedings of the 28th IEEE
EMBS Annual International Conference
New York City, USA, Aug 30-Sept 3, 2006

Physiologically Plausible Stochastic Nonlinear Kernel Models of Spike Train to Spike Train Transformation

Dong Song, *Member*, Rosa H. M. Chan, Vasilis Z. Marmarelis, *Fellow*, Robert E. Hampson, Sam A. Deadwyler, and Theodore W. Berger, *Member*, *IEEE*

***Abstract*—Nonlinear kernel models are developed and estimated for the spike train transformation from hippocampal CA3 region to CA1 region. The physiologically plausible model structure consists of nonlinear feedforward kernels that model synaptic transmission and dendritic integration, a linear feedback kernel that models spike-triggered after potential, a threshold, an adder, and a noise term that assesses the system uncertainties. Model parameters are estimated using maximum-likelihood method. Model goodness-of-fit is evaluated using correlation measures and time-rescaling theorem. First order, linear model is shown to be insufficient. Second and third order nonlinear models can successfully predict the output spike distribution.**

I. Introduction

ONE of the key components of hippocampus prosthesis project is the modeling of spatio-temporal pattern transformation [1], namely, predicting spike trains in the downstream region, e.g., CA1, based on spike trains in the upstream region, e.g., CA3. This model would potentially allow us to bypass the brain region damaged by diseases or injuries, and thus restore its cognitive functions. This paper describes a modified Volterra kernel approach for such task.

First, the modeling problem is formulated as the identification of a multiple-input-multiple-output (MIMO) system that could be broken down into a series of multiple-input-single-output (MISO) systems. Each MISO system is then modeled with a physiologically plausible structure that is able to differentiate and capture feedforward and feedback linear/nonlinear dynamics of the system (Fig. 1). Previous studies showed that a spike-triggered feedback component allows modeling of a variety of spiking behaviors omitted by purely feedforward models [2, 3]. Furthermore, to assess the spiking uncertainty and include contributions of unobserved inputs, a Gaussian noise term is added to the model.

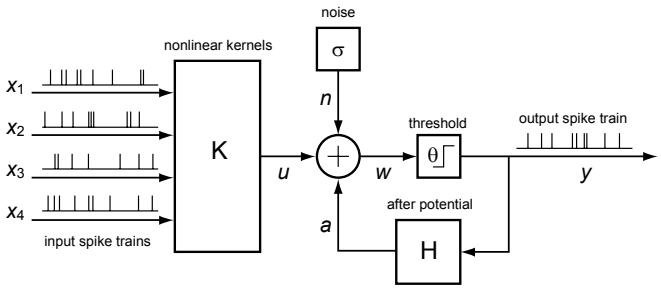

Fig. 1. General model structure.

II. Methodology

A. Experimental Procedures

Spike trains are recorded from rats performing delayed-nonmatching-to-sample (DNMS) task [4]. On each side of the brain, an array of 16 electrodes (microwires) is surgically implanted into hippocampus, with 8 in CA3 region and 8 in CA1 region. Each electrode can record up to 4 cells. Spike and behavioral responses are digitized and timestamped with a 25 μs resolution.

B. Data Preprocessing

Spike trains are selected based on their firing rates and perievent histograms. Neurons with (a) mean firing rate in the range of 0.5 to 15 Hz and (b) identifiable perievent histograms are kept for further analysis. Low (<0.5 Hz) and high (>15 Hz) rate recordings are rejected since they could be either artifacts or mixtures. To reduce data length, bin size is increased to 2 ms, which is still shorter than the neuron's refractory period. Finally, perievent (-2s to 2s) spike trains are extracted for each behavioral event and then concatenated. This procedure greatly reduces data length and allows future study of the relations between external events and spike train transformations.

C. Model Configuration

The general model structure consists of nonlinear

Manuscript received April 3, 2006. This work was supported by NSF, DARPA(HAND), and NIH(NIBIB).

D. Song is with the Department of Biomedical Engineering, Center for Neural Engineering, University of Southern California, Los Angeles, CA 90089 USA (phone: 213-740-8063; fax: 213-740-0343; e-mail: dsong@usc.edu).

H. M. Chan is with the Department of Biomedical Engineering, University of Southern California, Los Angeles, CA 90089 USA (e-mail: homchan@usc.edu).

V. Z. Marmarelis is with the Department of Biomedical Engineering, Center for Neural Engineering, University of Southern California, Los Angeles, CA 90089 USA (e-mail: vzm@bmsr.usc.edu).

R. E. Hampson is with the Department of Physiology & Pharmacology, Wake Forest University, School of Medicine, Winston-Salem, NC 27157 USA (e-mail: rhampson@wfubmc.edu).

S. A. Deadwyler is with the Department of Physiology & Pharmacology, Wake Forest University, School of Medicine, Winston-Salem, NC 27157 USA (e-mail: sdeadwyl@wfubmc.edu).

T. W. Berger is with the Department of Biomedical Engineering, Program in Neuroscience, Center for Neural Engineering, University of Southern California, Los Angeles, CA 90089 USA (e-mail: berger@bmsr.usc.edu).

feedforward kernels K, a linear feedback kernel H, a threshold, an adder, and a Gaussian white noise with standard deviation σ (Fig. 1). K models the nonlinear dynamics of synaptic transformation and dendritic integration. H models the spike-triggered "after-potential". A spike is generated when the hidden variable *w* crosses threshold. The noise term models the intrinsic noise of the neuron, and more importantly, unobserved input signals.

The model can be expressed by the following equations:

$$w = u(\vec{k}, \vec{x}) + a(\vec{h}, \vec{y}) + n(\sigma) \tag{1}$$

$$y(w) = \begin{cases} 0 & \text{when } w < \theta \\ 1 & \text{when } w \geq \theta \end{cases} \tag{2}$$

where *x* are input spike trains, *y* is output spike train, *n* is a Gaussian white noise with standard deviation σ, *u* is "synaptic potential", *a* is "after-potential", *w* is "subthreshold membrane potential". *k* are feedforward kernels. *h* is feedback kernel.

D. Parameter Estimation

Model parameters are estimated using maximum-likelihood method. The likelihood function could be expressed as:

$$L(\vec{k}, \vec{h}, \sigma, \theta) = \prod_i P(\vec{k}, \vec{h}, \sigma, \theta)_i \tag{3}$$

$$P_i(\vec{k}, \vec{h}, \sigma, \theta) = \begin{cases} \text{Prob}\,(w \geq \theta) & \text{when } t = spike \\ \text{Prob}\,(w < \theta) & \text{when } t \neq spike \end{cases} \tag{4}$$

t is actual output spike train. Model parameters *k*, *h*, and σ are estimated by maximizing the likelihood function *L*, given *x* and *t*. Laguerre expansion technique is used to decrease the number of parameters to be estimated [5-7]. Three Laguerre basis functions are used in most of the models.

E. Model Validation and Prediction

Model goodness-of-fit is assessed using Kolmogorov-Smirnov (KS) test based on the time-rescaling theorem [8]. More specifically, the time axis of output spike train (*t*) is rescaled using firing probability predicted by the kernel model. If the model agrees with the experimental data, the inter-spike intervals (ISI) are transformed into independent uniform random variables on the interval (0, 1), which could be easily evaluated with a KS plot.

Furthermore, the similarity between predicted output *y* and recorded output *t* is evaluated using Pearson correlation measures (*r*) after convolving them with Gaussian kernels with varying standard deviation σ_g.

III. Results

First, second, and third order kernel models are built and estimated using input-output spike trains (*x* and *t*). High order nonlinear terms being capable of capturing high order nonlinear dynamics are progressively included in K. H is fixed to be linear (first order) in all models.

A. First Order Kernel Model

K is linear in the first order model (Fig. 2 and 3). Four input spike trains are included (Fig. 2 left).

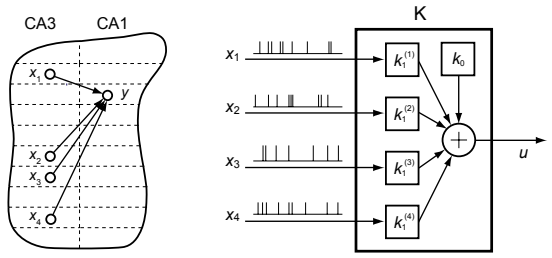

Fig. 2. K of first order kernel model and recording sites.

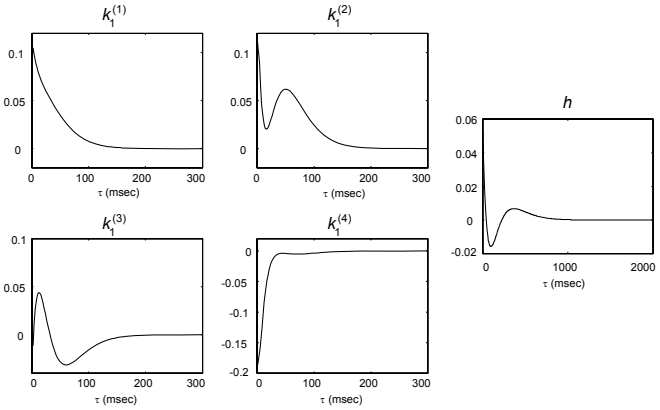

Fig. 3. First order kernel model ($\sigma = 0.32$).

The KS plot shows that there is lack of fit at lower half of quantiles (0.2-0.6), because in that range, its values lay outside the 95% confidence bounds (Fig. 11 right).

B. Second Order Self Kernel Model

Second order self kernel model has second order terms for each individual input. It is built with 3 inputs (Fig. 4).

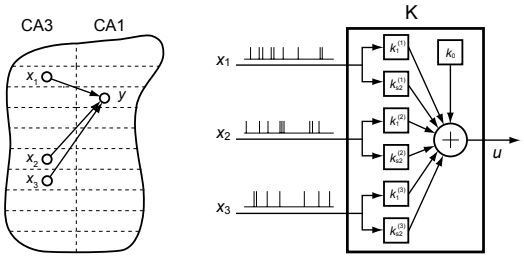

Fig. 4. K of second order self kernel model and recording sites.

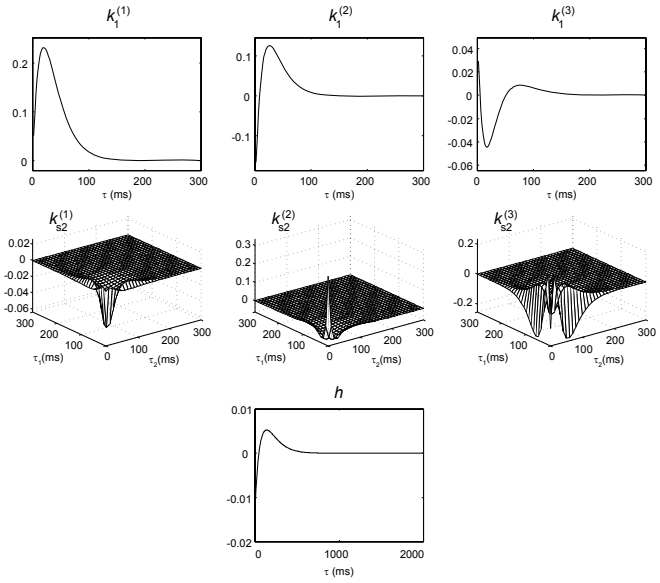

Fig. 5. Second order self kernel model ($\sigma = 0.30$).

C. Second Order Self and Cross kernel Model

Second order self and cross kernel model has additional cross terms modeling the interactions between inputs. It is built with 2 inputs (Fig. 6 and 7).

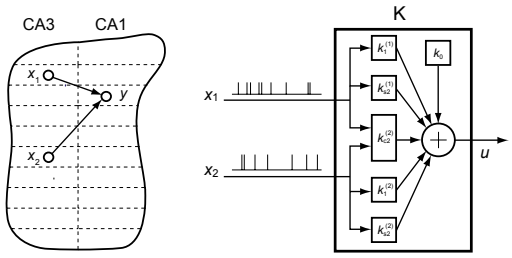

Fig. 6. K of second order self and cross kernel model and recording sites.

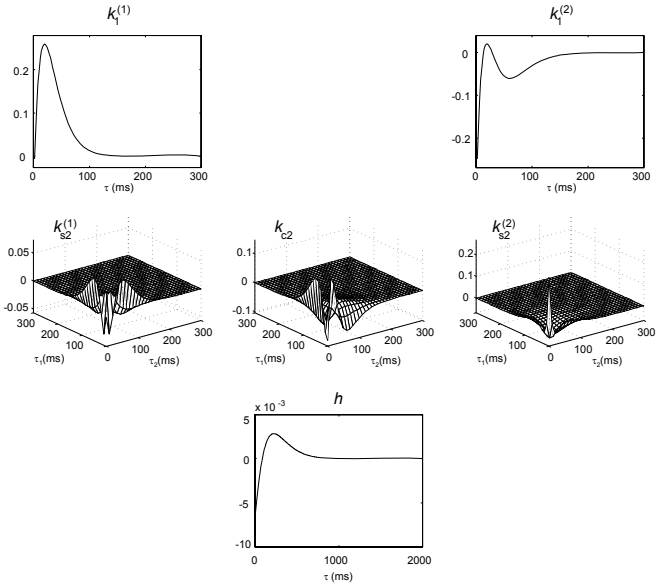

Fig. 7. Second order self and cross kernel model ($\sigma = 0.30$).

D. Third Order Self Kernel Model

Third order self kernel model is also built with 2 inputs (Fig. 8). It has additional third order terms for each input, but no cross terms (Fig. 8 and 9).

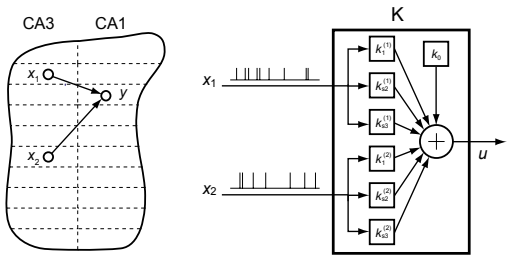

Fig. 8. K of third order self kernel model and recording sites.

All three nonlinear models above successfully fit the data in the whole range of quantiles (Fig. 11), i.e., their KS plots well match the 45 degree lines and lay inside the 95% confidence bounds in the entire range from 0 to 1. These results show that the transformation of input spike train x to "membrane potential" w is nonlinear and thus nonlinear kernel models are required.

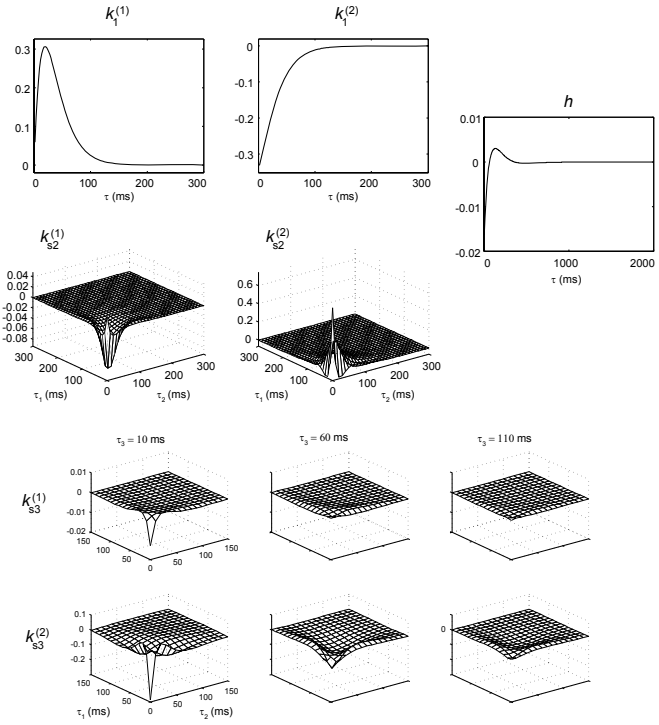

Fig. 9. Third order self kernel model ($\sigma = 0.30$).

E. Model Prediction

The kernel models described in this paper predict output spike trains stochastically due to their noise terms. They not only model the output spiking probability, but also assess the uncertainty of spike generation. Figure 10 showed two trials of simulation with identical input spike trains. The simulated outputs showed similar but different patterns in each trial.

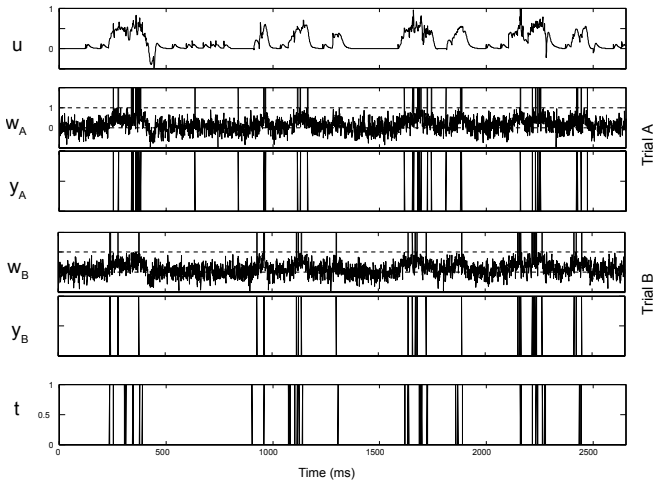

Fig. 10. Two trials of model prediction using second order self and cross kernel model.

Consistent with KS plot results, both correlation measure (Fig. 11 left-bottom) and likelihood results (Fig. left-top) show that nonlinear kernel models are significantly more accurate than the linear kernel model.

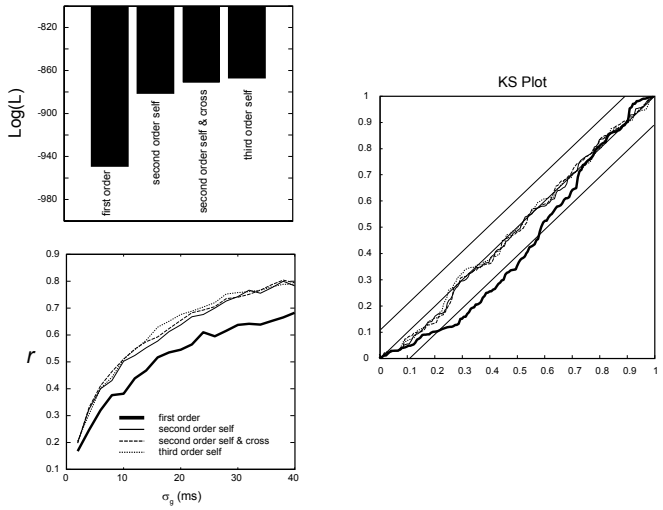

Fig. 11. Likelihood (Left-top), coefficients of correlation (Left-bottom) and KS plots (Right) with different model orders.

IV. Discussion

Physiologically plausible models are successfully developed and estimated for the CA3 spike train to CA1 spike train transformations during DNMS task. Our results show that these transformations have significant nonlinearities that require at least second order feedforward kernels. Second order self, second order self and cross, and third order kernel models give comparably good fit to the output spike trains.

Given the same output, CA3 neurons exhibit different forms of nonlinear dynamics represented by different kernel shapes (Fig. 3, 5, 7, 9). An interesting follow-up study would be systematically exploring this functional heterogeneity and associating it with the anatomical, physiological, and other functional properties of the neurons, e.g., relating functional cell types to kernel shapes.

In the current model, intrinsic neuronal noise and unobserved inputs are modeled as a Gaussian white noise. Adding noise component has the following important consequences: first, model predictions become stochastic. It is more appropriate to evaluate the model goodness-of-fit with respect to its output statistical properties, e.g., ISI distributions; 2) maximum-likelihood function (L) could be formulated to estimate the model parameters. The calculation of L involves error function, i.e., integral of Gaussian function, and thus could not be reduced to least-squares linear regression estimation.

The whiteness assumption to the noise could be inaccurate under some circumstances, e.g., when the input spike trains are weakly correlated to the output spike train. We conceive of using noise kernel(s) to model the correlated noise. Further work needs to be done to address this issue.

In the current model configuration scheme, MIMO system is modeled as a series of MISO systems. This strategy works well with our current input-output datasets but could become inefficient when there are a large number of correlated outputs. We are currently developing a canonical correlation analytical approach to solve this problem.

Acknowledgment

R. H. M. Chan thanks Croucher Foundation and Sir Edward Youde Memorial Fund for the fellowship supports.

References

[1] T. W. Berger, A. Ahuja, S. H. Courellis, S. A. Deadwyler, G. Erinjippurath, G. A. Gerhardt, G. Gholmieh, J. J. Granacki, R. Hampson, M. C. Hsaio, J. LaCoss, V. Z. Marmarelis, P. Nasiatka, V. Srinivasan, D. Song, A. R. Tanguay, and J. Wills, "Restoring lost cognitive function," *IEEE Engineering in Medicine & Biology Magazine*, vol. 24, pp. 30-44, 2005.

[2] L. Paninski, J. W. Pillow, and E. P. Simoncelli, "Maximum likelihood estimation of a stochastic integrate-and-fire neural encoding model," *Neural Computation*, vol. 16, pp. 2533-61, 2004.

[3] J. Keat, P. Reinagel, R. C. Reid, and M. Meister, "Predicting every spike: a model for the responses of visual neurons," *Neuron*, vol. 30, pp. 803-17, 2001.

[4] R. E. Hampson, J. D. Simeral, and S. A. Deadwyler, "Distribution of spatial and nonspatial information in dorsal hippocampus.," *Nature*, vol. 402, pp. 610-4, 1999.

[5] D. Song, Z. Wang, V. Z. Marmarelis, and T. W. Berger, "Nonparametric interpretation and validation of the parametric short-term plasticity models," in *Proc. 25th Annu. EMBS Conf.*, 2003, pp. 1901-4.

[6] D. Song, V. Z. Marmarelis, and T. W. Berger, "Parametric and non-parametric models of short-term plasticity," in *Proc. 2nd Joint EMBS/BMES Conf.*, 2002, pp. 1964-5.

[7] V. Z. Marmarelis, "Identification of nonlinear biological systems using Laguerre expansions of kernels," in *IEEE Transactions on Biomedical Engineering*, vol. 40, 1993, pp. 1149-58.

[8] E. N. Brown, R. Barbieri, V. Ventura, R. E. Kass, and L. M. Frank, "The time-rescaling theorem and its application to neural spike train data analysis," *Neural Computation*, vol. 14, pp. 325-46, 2002.